# A REVIEW OF COMPUTATIONAL CERAMIC ARMOR MODELING

Charles E. Anderson, Jr.
Southwest Research Institute
P.O. Drawer 28510
San Antonio, TX 78228-0510

## ABSTRACT

Computational ceramic armor models are reviewed, with an emphasis on a historical perspective. Some discussion concerning the current state of the art is provided, including a summary of issues concerning the strength of *in-situ* comminuted ceramic.

## INTRODUCTION

Focused sessions on armor ceramics became part of the *International Conference & Exposition on Advanced Ceramics & Composites* annual meetings in 2003. Each year, the Organizers of these focused sessions have selected a topic area and presenter for the first (keynote) talk to start the conference, with the objective of providing an historic overview of some aspect of armor ceramics. Computational ceramics armor modeling was the focused topic for the 2005 meeting. This article documents the presentation that was made at that meeting. The article does not provide an exhaustive review of all the work done in this area, but it does highlight significant progress and difficulties in computational ceramic modeling.

## THE LIGHT ARMOR PROGRAM

Mark Wilkins developed the first computational ceramic armor model, circa 1968, as part of the multi-year light armor program, funded by DARPA, to defeat rifle-fired, armor-piercing (AP) bullets [1-5]. Weight is always an issue with armor, so materials are pushed to their limit, that is, failure. As Wilkins stated: "The application of materials to light armor is unusual because material properties are utilized in the region of material failure, i.e., if the armor doesn't fail for a given ballistic threat, it could be made lighter" [3]. Numerical simulations were an integral portion of the light armor program, providing illumination and guidance.

Early on in the light armor program, Wilkins realized that a lightweight system had requirements for different, and conflicting, material properties. A hard element is needed to erode and decelerate the bullet. A ductile element is required to capture the remnants of the eroded bullet. Thus, materials with different properties need to be assembled in the most advantageous way. Photographs of an experiment, Fig. 1, conducted at Southwest Research Institute (SwRI) depict the response of an AP bullet against a $B_4C$ ceramic tile glued to an aluminum (6061-T6) substrate. The front view shows the damage to the ceramic, and the side view shows the deformation of the aluminum substrate plate. Horizontal lines were drawn on the back of the substrate plate to assist in visualizing the deformation. As can be seen, the substrate plate absorbs some of the kinetic energy through deformation.

Wilkins conducted simulations into metallic targets [1] prior to investigating ceramics. The threat bullet was the 7.62-mm armor-piercing APM2. However, Wilkins developed a monolithic 0.30-cal bullet as a surrogate projectile for the APM2 bullet, largely to decrease the scatter in experimental data resulting from fracturing of the hard steel core in the APM2 bullet. Muzzle velocity for the bullets is 820-850 m/s. The physical characteristics of these two bullets

are summarized in Table I, and schematics of the bullets are shown in Fig. 2. The surrogate bullet has a penetration performance similar to that for the APM2 bullet into hard targets.

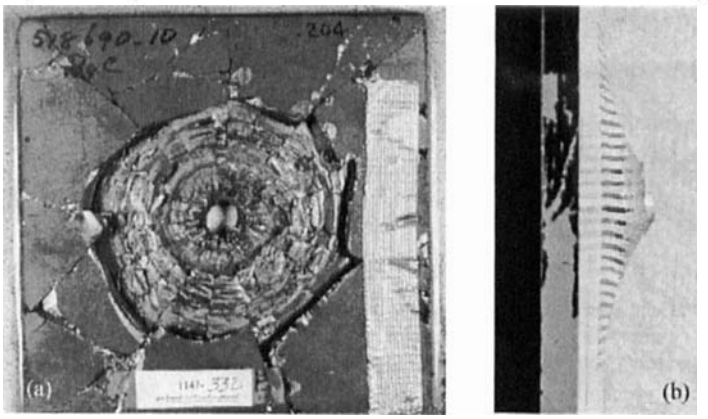


Fig. 1. Post-test photograph of impact of AP bullet against ceramic/aluminum target: (a) front view of ceramic element; (b) side view of target showing deformation of aluminum element.

Table I. Physical Properties of the 7.62-mm AP Bullets

| 7.62-mm APM2 Bullet | 7.62-mm Surrogate AP Bullet |
|---|---|
| Mass: 10.74 g | Mass: 8.32 g |
| Length: 3.53 cm | Length: 2.81 cm |
| Core Mass: 5.25 g | Nose: 55° cone |
| Core Length: 2.74 cm | Hardness: $R_c$ 55 |
| Core Hardness: $R_c$ 62-65 | |

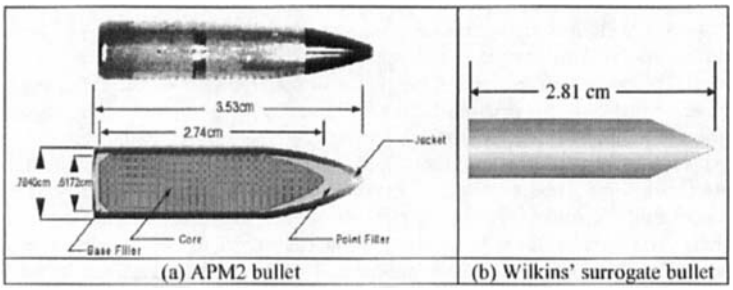


Fig. 2. 7.62-mm (0.30-cal) bullets of the ight armor program.

This activity took place during the days of (Hollerith) computer cards, one of which is shown in Fig. 3. Holes, representing a line of a FORTRAN code were punched into these cards; "fingers" read the punched holes when fed into a card reader. Two thousand cards came in a box, and a large program like HEMP required 3 to 5 boxes for the entire program. (It is noted

that it was a "bad" day when a box of cards was dropped, and a *very* bad day if the cards weren't sequenced in columns 73-80).

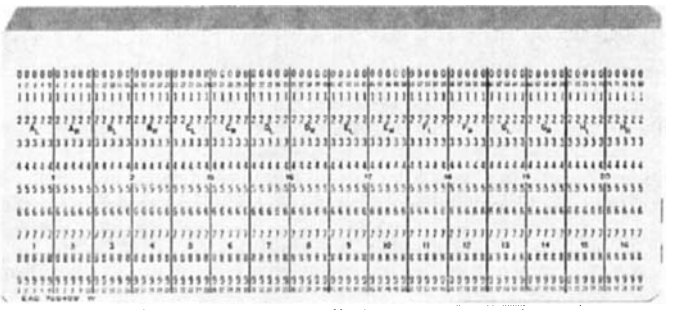

Fig. 3. 80-column Hollerith computer card.

Constraints on Modeling

Before proceeding, it is useful to describe constraints that are imposed on a model if the model is to assist in understanding and/or design. It must be demonstrated that the model captures essential features of observed phenomena, and it must be demonstrated that the model provides reasonable agreement with experimental data. Otherwise, there can be no confidence in any predictions of the model. Further, model parameters should be connected to physical parameters (material properties), and if possible, these physical parameters should be determined from independent laboratory experiments. As will be seen, however, it is sometimes necessary to conduct parametric simulations and determine a value for a model parameter through matching to ballistic experiments. Finally, the same set of parameters should be applicable to a variety of types of experiments.

The above constraints may seem obvious; however, the field is littered with assertions of modeling successes, but only because model parameters were adjusted to replicate an experimental results. This is "self-consistency." Self-consistency is a necessary, but not a sufficient, condition for the validity of a model. This is why, for ballistics impact, it must be demonstrated that the same set of parameters is applicable over a range of impact velocities.

Wilkins' Ceramics Model

The ceramics model developed by Wilkins is applicable to thin (on the order of a projectile diameter) ceramic tiles. The model was implemented in the two-dimensional finite difference code HEMP [6-7]. A primary emphasis of the model was to simulate the development of the fracture conoid, which was observed in experiments. It took until Model 17 before Wilkins was satisfied that he had something that represented the behavior of a ceramic tile to impact [8].*

The Wilkins' ceramic model is a tensile failure model. When the maximum principal stress of a cell exceeds a tensile stress criterion ($\sigma > \sigma_f$), where the stress is positive in tension, fracture is initiated within the computational cell (see Fig. 4). But additional criteria had to be applied, otherwise all the zones tended to fail within a few computational cycles. An internal

* I do not remember whether it was really Model #17 or another (fairly large) number. The important point is that it took a while before Wilkins felt that simulations using the model replicated experimental reality.

state variable $\varphi_f$ is used to track damage within a computational cell. Once initiated, fracture is assumed to propagate through the cell at some fraction of the shear wave speed, specified by the parameter $f_1$ (see Fig. 5). Also, once fracture is initiated, the fracture continues within the cell until complete, that is, $\varphi_f$ starts at 0 and fracture continues until $\varphi_f$ = 1. As the damage propagates, the cell is progressively weakened, as given in Fig. 5. Thus, it takes a finite amount of time (the time it would take a crack—moving at some fraction of a shear wave—to propagate across a characteristic dimension of the computational cell) before the cell has completely fractured.

An additional fracture initiation criterion also had to be implemented: fracture initiation of a computational cell could only occur at surfaces (including material interfaces) or if a neighboring (immediately adjacent) cell had completely fractured, $\varphi_f$ = 1, subject to the criterion that $\sigma > \sigma_{f^*}$ at the specified computational time step. In this manner, damage propagated on the computational grid like a crack, at a fraction ($f_1$) of the shear wave velocity. It is important to note that damage (fracture) will arrest if the tensile stress is less than the tensile stress fracture criterion $\sigma_{f^*}$.

- Fracture initiates on surfaces where the maximal principal stress is greater than $\sigma_{f^*}$: $\sigma > \sigma_{f^*}$ (stress is positive in tension)
- A fracture may also initiate within a cell if the maximal principal stress is greater than $\sigma_{f^*}$ ($\sigma > \sigma_{f^*}$) and a neighboring cell has completely fractured, i.e., $\varphi_{f_{neighbor}} = 1$

Fig. 4. Wilkins' ceramic model: fracture initiation criteria.

- The ceramic material has a parameter $\varphi_f$: $0 \le \varphi_f \le 1$

  $\varphi_f = 0$ no fracture has occurred

  $\varphi_f = 1$ material in cell is completely fractured
- If a cell has fractured, it continues to fracture until fracture is complete

  $\varphi_f^{n+1} = \varphi_f^n + \Delta\varphi_f$ until $\varphi_f^{n+1} = 1$

  where

  $$\Delta\varphi_f = f_1 \frac{C_{shear} \bullet \Delta t^n}{X} \qquad 0 < f_1 \le 1$$

  $C_{shear} = \sqrt{G/\rho} \equiv$ shear wave speed

  $X$ = characteristic length of cell $\left(e.g., X = \sqrt{(\Delta x)(\Delta y)}\right)$
- Cell progressively softens during fracture:

  $Y = (1 - \varphi_f) Y_{intact}$

Fig. 5. Wilkins' ceramic model: fracture propagation with a cell and cell strength.

The Wilkins' ceramic model was implemented into an early version of CTH [9-10]. To examine some essential results using the Wilkins' model, a simulation of the 7.62-mm AP simulant impacting a 7.62-mm-thick $B_4C$ tile glued to a 6.35-mm-thick 6061-T6 aluminum

substrate was conducted. The ballistic limit for this target is 820 m/s [3]. The results for early time steps are shown in Fig. 6. A fracture conoid begins within the first few microseconds after impact. At approximately 5 μs, an axial crack is initiated at the ceramic-aluminum interface. The fracture conoid proceeds toward the substrate and effectively limits the amount of ceramic that participates in the impact process. The axial crack moves back toward the impact surface, and by 10 μs, the ceramic underneath the penetrator has completely failed.

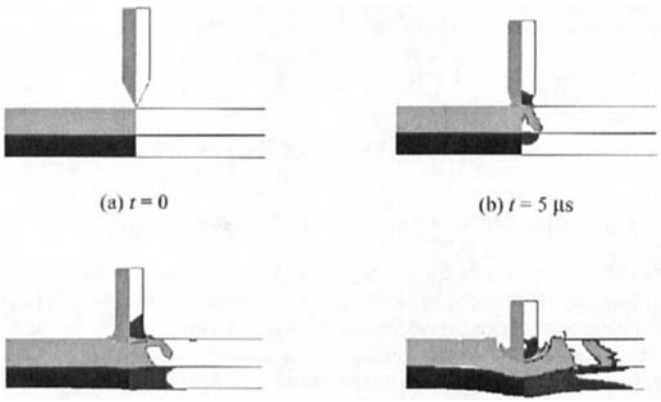


Fig. 6. Simulations results for the impact of an AP projectile into a $B_4C$/Al target using the Wilkins' ceramic model.

The computational results are very zone-sized dependent because of the stress-dependent initiation criterion. Wilkins used 40 zones across the radius of the projectile [8]. Even with today's computational power, 40 zones across the radius of the projectile is a very large number (5 to 10 zones across the radius are typical numbers for many 2-D simulations). Circa 1968, 40 zones to resolve the radius was a phenomenally large number. To put this in perspective, with 40 zones across the radius of the bullet, then there were approximately 17,700 computational cells in the problem (assuming nominally square zoning). The time step is proportional to the smallest zone dimension divided by the material sound speed, and since the sound speed of ceramics is very high (~10 km/s for $B_4C$), this gives a maximum time step of 0.01 μs. The "grind time" (the amount of computer time per zone per time step) for the supercomputers at that time was on the order of 1 ms per zone cycle. Since HEMP is a Lagrangian code, zonal distortion limited the time step even further. Wilkins carried his calculations out for ~1400 cycles (~6 μs), which took about 6-7 hours CPU time to reach 6 μs; wall clock time was probably significantly longer.

## MODIFIED WILKINS' CERAMIC MODEL

In 1991, Walker and Anderson [9] placed the Wilkins' model into CTH [10] and reproduced Wilkins' results. Starting about 1996, the model was used extensively in the DARPA/Army ultra-lightweight body armor program. The failed ceramic material in the

original Wilkins' model did not have strength. (Wilkins surely added this later, but the strength of the failed material is not mentioned in the description of the model that is summarized in his reports [3-4].) We found that the failed material had to have some sort of strength; else, the bullet easily perforated the target with a significant amount of its original kinetic energy [11]. Thus, the first modification to the Wilkins' ceramic model was to model the failed ceramic material with a Drucker-Prager model, characterized by a slope $\beta$ and a cap $\bar{Y}$. When fracture was initiated within a computational cell (applying the same initiation and propagation criteria as specified in Figs. 1 and 2), the cell strength went from that of an intact material to failed material, as summarized in Fig. 7, as $\varphi_f$ transitioned from 0 to 1.

$$Y = (1-\varphi_f)Y_{\text{intact}} + \varphi_f Y_{\text{fail}}$$

$$Y_{\text{fail}} = \begin{cases} 0 & P < 0 \\ \beta P & 0 \le P \le \bar{Y}/b \\ \bar{Y} & P \ge \bar{Y}/b \end{cases}$$

Fig. 7. Modified Wilkins' ceramic model: strength after fracture.

The penetration-time results for an impact of 820 m/s (the ballistic limit determined by Wilkins) are shown in Fig. 8, using values of $\beta = 1.4$ with no cap to limit the flow stress. This actually looks quite good. Since approximately 40% of the core is eroded in the simulation, the residual kinetic energy is ~0.50% of the initial kinetic energy. Although this would appear to be very good agreement, the model could not reproduce a number of experimental observations: it did not provide good estimates of residual velocities for overmatched impact conditions, it did not provide good estimates of residual projectile length, and it did not adequately predict dwell.

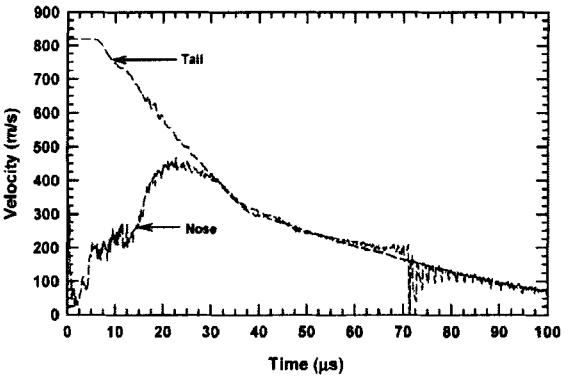


Fig. 8. Nose and tail velocities for 0.30-cal simulant into $B_4C$/6061-T6 aluminum target.

Hundreds of computer simulations were conducted, varying the parameters in the modified Wilkins' model. Particularly useful data were the residual length of the cores of the APM2 bullet, Fig. 9, since the core is only eroded by the ceramic (the core penetrates the aluminum substrate as a rigid body). Other very useful data were tests conducted for SwRI by the Army Research Laboratory using their 1-MeV flash X-ray system [12]. The targets, 7.62-mm $B_4C$ tiles glued to 6.6-mm 6061-T6 aluminum substrates, were fabricated at SwRI. Three of the

radiographs are shown in Fig. 10 at different times after impact. Dwell persists for approximately 20 μs; the bullet is just beginning to penetrate into the ceramic in Fig. 10(b). In order to match the various experimental data, the parameter $f_1$ in the Wilkins' model had to be decreased from 0.5 to 0.025. This parameter is associated with how fast the damage propagates through a computational cell. The original interpretation was that a crack propagated at some fraction of the sound speed. But to match the experimental data, $f_1$ had to be reduced by a factor of 20. This low value for $f_1$ was interpreted as the time it takes to comminute the ceramic. Hence, the somewhat now famous expression—"Cracks don't matter!"—which was uttered by the author at a ceramics workshop held at the Institute for Advanced Technology circa 1998. A comparison of the damage at 5 μs after impact for the two values of $f_1$ is shown in Fig. 11.

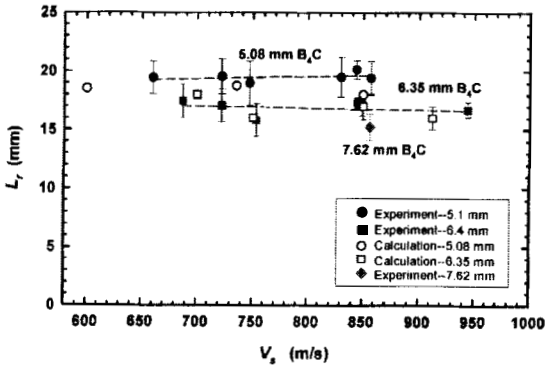


Fig. 9. Length of core as a function of impact velocity and ceramic tile thickness.

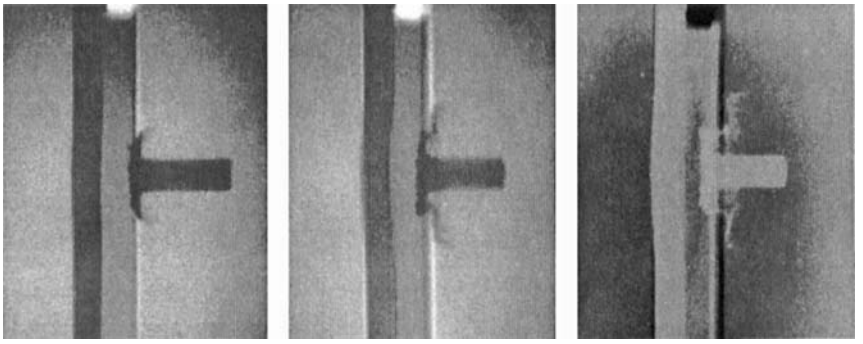

(a) $t$ = 15.3 μs ($V_s$ = 825 m/s) (b) $t$ = 20.7 μs ($V_s$ = 819 m/s) (c) $t$ = 22.9 μs ($V_s$ = 827 m/s)

Fig. 10. Flash radiographs of APM2 impacting a 7.62-mm $B_4C$/6.6-mm 6061-T6 Al target at approximately 825 m/s [12].

A comparison of a CTH simulation using the modified Wilkins' model to the data from the ARL experiments is shown in Fig. 12. The solid lines are the results of the simulation, and the

solid points are the positions of various surfaces or interfaces measured from the flash radiographs. Agreement is very good.

So what had we learned about ceramics modeling, at least for relatively thin tiles backed by a ductile substrate material? Firstly, it is necessary to have a description of the strength of the failed material if the experimental data are to be reasonably reproduce; and secondly, it is the comminution of the ceramic—not crack propagation—that is important for local penetration.

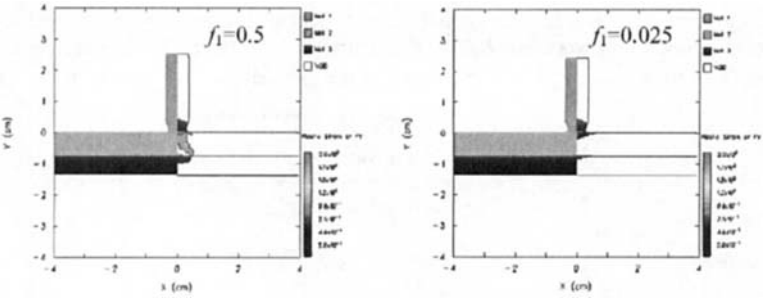


Fig. 11. Comparison of damage profiles at 5 μs for different values of $f_1$.

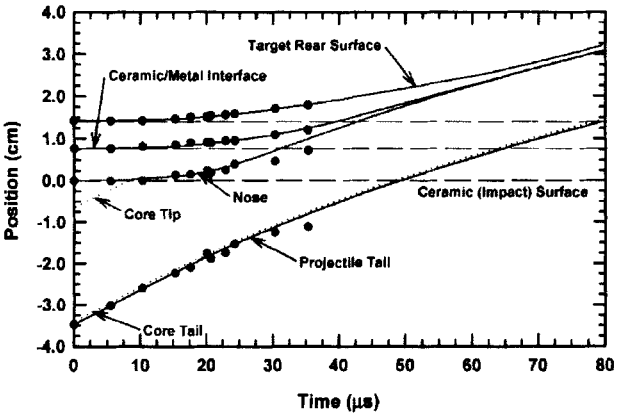


Fig. 12. Position-time for APM2 bullet impacting $B_4C$/6061-T6 target [12].

## OTHER COMPUTATIONAL CERAMICS MODELS

The Wilkins (1968) and the modified Wilkins' ceramic models (1997-'98) are a tensile failure model, and are applicable to thin ceramic tiles. Rajendran [13] provides an excellent overview of other computational ceramic models. Only two will be discussed here—the Rajendran-Grove model and the Johnson-Holmquist model—but with more emphasis on the latter model. In the 1989-1990 timeframe, two ceramic models were developed, one by Rajendran, and the other by Johnson and Holmquist. The Rajendran-Grove model, based on micro-mechanics, degrades the elastic constants as damage accumulates in the form of

microcracks [14-17]. Microcrack damage is measured in terms of a dimensionless microcrack density; the evolution law for growth/extension of the microcracks is derived from fracture mechanics and is based on a relationship for a single crack propagating under dynamic loading conditions. The ceramic "softens" (the elastic constants are degraded) as a function of the dimensionless microcrack density until some critical value of damage is reached, whereupon, the response is characterized by completely failed material. Prior to pulverization, the model also allows for pore collapse—to account for initial porosity in the intact ceramic—during compressive loading due to local microplastic flow of the matrix material surrounding the pores. Rajendran initially was interested in reproducing wave profiles from shock-wave (uniaxial strain flyer-plate) experiments,** but later began to apply the model to penetration, e.g., Ref. [14,17].

There was emphasis in using ceramics for heavy armor under the auspices of the DARPA heavy armor research initiative in the mid to late 1980's. Johnson and Holmquist developed a phenomenological computational ceramics model [18] under this effort, including how to determine constitutive constants [19]. The Johnson-Holmquist (J-H) model describes the "yield surface" for inelastic strain. The strengths of the intact and failed materials are functions of the confining pressure. The transition from intact to failed material is dependent on accumulated inelastic strain, which is also a function of pressure. Today, the J-H model is probably the most widely used computational ceramics model, although the form of, and the constants used in, the J-H model have evolved (and continue to evolve) [20-25]. The most recent model is shown in Fig. 13. The left-hand figure shows the equivalent stress for the intact and failed material as a function of confining pressure at two strain rates. The accumulation of damage, as measured by plastic strain, is shown in the top right figure. Bulking is denoted by the bottom right figure.

An analytical ceramics model was developed in 1996 for application to thin tiles [26]. The model assumes that the material being penetrated has failed and can be described by a Drucker-Prager yield surface. Two regions are envisioned: an inner region described by a pressure-dependent yield surface, which is surrounded by intact material (the second region). This required solution of an integral equation to define the boundary between the two regions. Further development of the model added a cap, which then required an interior boundary solution [27]. The pressure-dependent region corresponds to comminuted pieces sliding over each other; the cap corresponds to material-deforming plastic flow. The model was applied to long-rod penetration into semi-infinite ceramic targets [28-30]. Although this model is an analytical, in contrast to a computational, constitutive model, it is described here because it highlights one of the most pressing issues in computational ceramic modeling, which is the strength of the failed ceramic, the topic of the next section.

## THE FAILED SURFACE

The constitutive form for the response of the failed material—a Drucker-Prager model—is common to all the models described above. Clearly, then, the response of the failed material is an extremely important aspect of any ceramic model. Walker took the constitutive constants for $B_4C$, as determined for the modified Wilkins' model from 100's of CTH simulations, and calculated the penetration of tungsten long rods into semi-infinite $B_4C$ targets as a function of impact velocity. The constitutive constants used were the slope $\beta = 1.7$ and the cap $\bar{Y} = 4.0$ GPa. The model results are compared to experimental data by Orphal, *et al.* [31] in Fig. 14.

** It was quickly learned that matching shock-wave profiles, although a necessary condition for the models, is not sufficient. Shock-wave profiles are insensitive to variations in some of the constitutive parameters; whereas, these parameters can be very important in penetration problems.

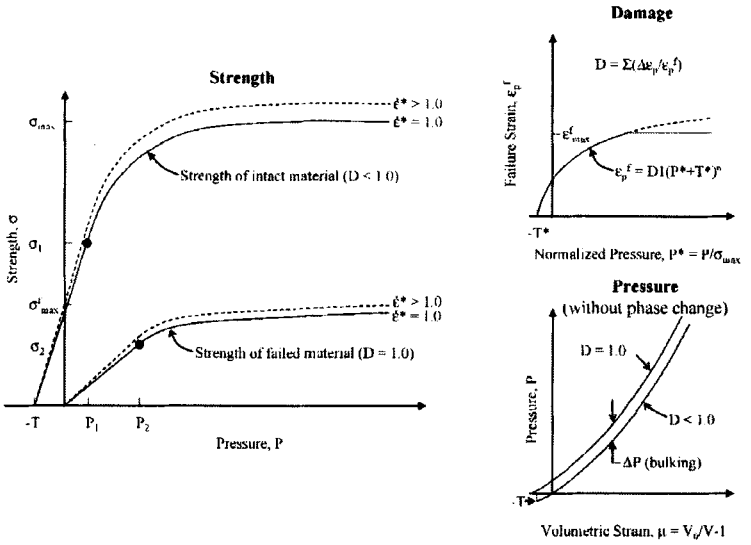


Fig. 13. Johnson-Holmquist-Beissel (JHB) model [25] (courtesy of T. Holmquist).

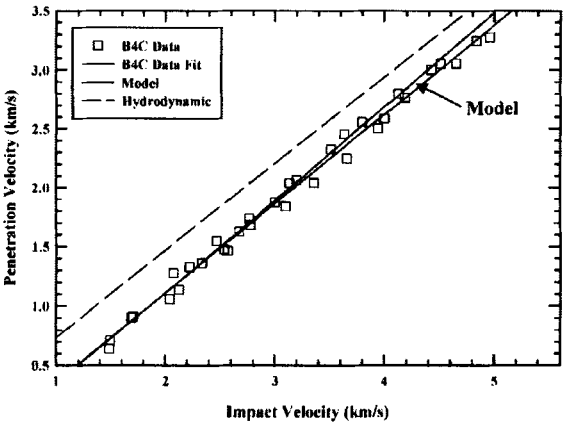


Fig. 14. Tungsten into $B_4C$: comparison of the Walker-Anderson ceramics model to experimental data from [28].

Agreement is quite good, except for the highest impact velocities. Earlier, during the ultra-lightweight armor program (but independent of the Wilkins' model calibration effort), Johnson and Holmquist developed constitutive constants for $B_4C$ for a slightly revised version of the J-H model (JH-2), which uses analytic equations to describe the yield surfaces. The equivalent stress vs. pressure for the intact and failed surfaces are shown in Fig. 15. The Drucker-Prager model parameters used by Walker are also plotted in the figure. The agreement between the J-H model

parameters and those used by Walker are in very good agreement, although the actual position of the cap is in the "eye of the beholder." It was very satisfying that the constitutive parameters inferred from CTH simulations agreed so well with the experimental data from Wilkins, and Mayer and Faber, for failed material.*** To place these results in historical perspective, the modified Wilkins' parameters were determined in 1997-'98, the JH-2 model parameters were developed in 1998-'99, and the Walker results, 2002.

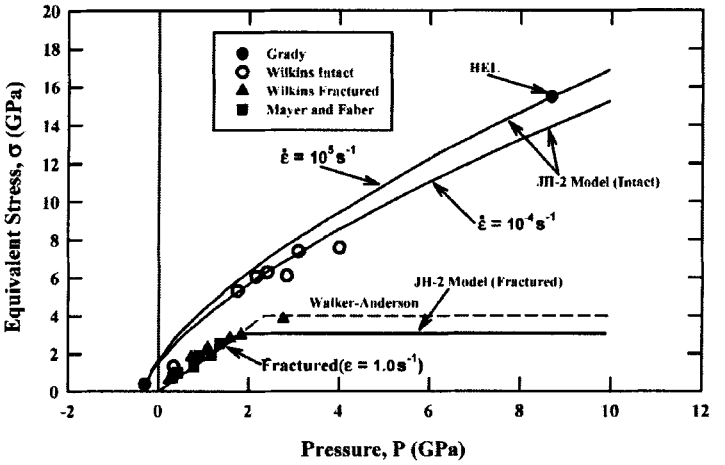


Fig. 15. JH-2 $B_4C$ model [21] with Walker-Anderson failure surface (JH-2 model courtesy of T. Holmquist).

Walker determined the Drucker-Prager constitutive parameters for SiC by conducting parametric studies and comparing the results to experimental data of tungsten long rods impacting semi-infinite SiC targets [32]. He determined that the constitutive should be: $\beta = 2.5$; $\overline{Y}$ = 3.7 GPa. Results are shown in Fig. 16. Further, he demonstrated that the slope and the cap were important, as shown in Fig. 17 [29]. The slope affects the penetration response (as compared to solely a constant flow stress) at the lower impact velocities, while the cap limits the effect of large penetration pressures at the higher impact velocities.

Holmquist and Johnson determined parameters for SiC [22], using the JH-1 model; the results are shown in Fig. 18. As there were no data for failed SiC material, they inferred the strength from some ballistic experiments, to be described in a few paragraphs. The J-H parameters for the failed material are: $\beta = 0.40$, $\overline{Y}$ = 1.3 GPa. The description of the failed surface for the J-H model and the Walker-Anderson model are drastically different, as shown in Fig. 18. The time frame for the J-H results for SiC is 2001-'02.

*** Because of the analytic form of the JH-2 model, the slope is not singled valued, but $\beta \approx 1.9$, compared to 1.7 for the Walker-Anderson (and modified Wilkins') model. The cap is 3.09 GPa in the JH-2 model.

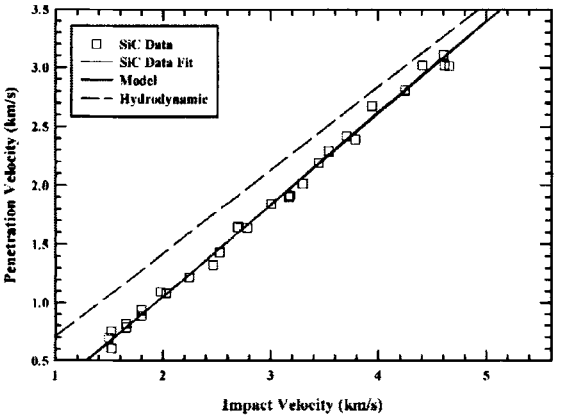


Fig. 16. Tungsten into SiC: comparison of the Walker-Anderson ceramics model to experimental data from [30].

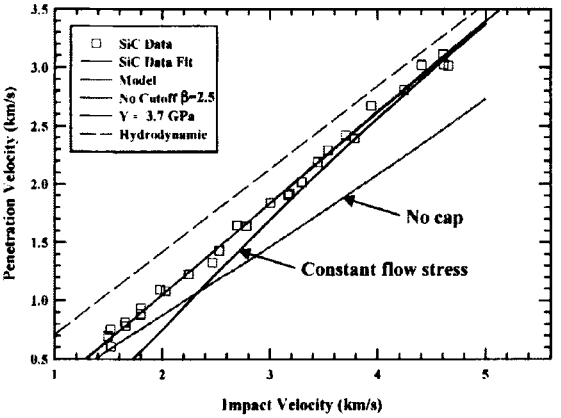


Fig. 17. Tungsten long rod into SiC: effect of slope and cap on model results [29].

But it gets worse! Some major enhancements were made to the J-H model. First, an algorithm for converting failed elements to generalized particles was developed, which suppressed numerical "noise" and maintained pressure at contact boundaries [33]. Additionally, they developed a capability to put a ceramic target under a state of prestress [24].**** These capabilities had a dramatic influence on the magnitude of the cap for the failed surface.

With the new capabilities, Holmquist and Johnson [25] re-examined experiments conducted by Lundberg, *et al.* [37]. These experiments, done in the reverse ballistics mode, involve launching highly confined ceramic targets at a very long (80-mm length, 2-mm diameter)

**** Another capability added is the ability to treat solid-solid phase transitions [34-36]

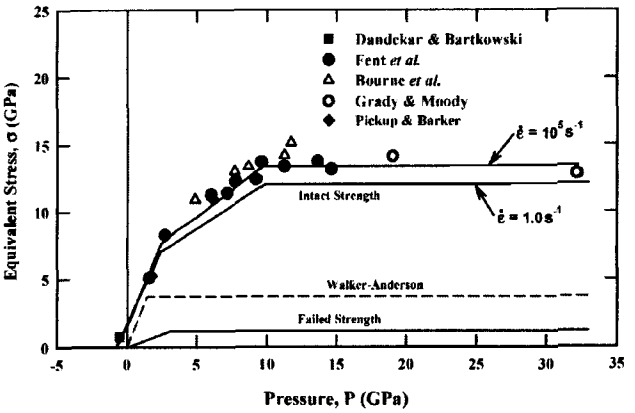


Fig. 18. Original J-H SiC model [22] with Walker-Anderson failure surface (J-H model courtesy of T. Holmquist).

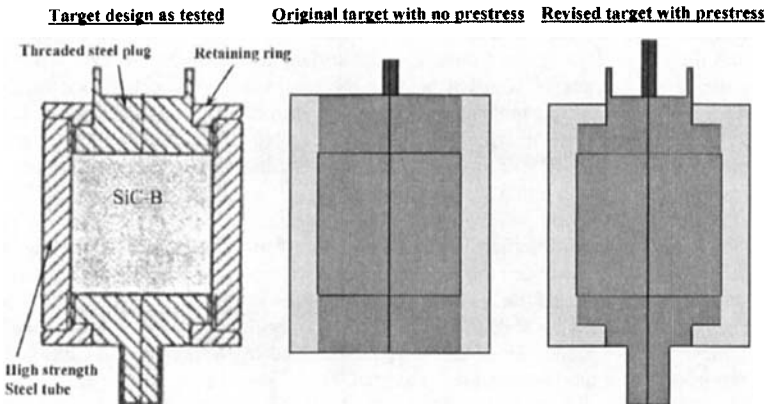


Fig. 19. Lundberg's target geometry (courtesy of T. Holmquist).

tungsten-alloy penetrator. The Lundberg target is shown on the left-hand side of Fig. 19; the SiC-B designation denotes a specific type of silicon carbide manufactured by Cercom. In the original work [22], Holmquist modeled the target as shown in the center figure of Fig. 19. In the more recent work [25], the geometric description of the target has higher fidelity, and included a prestress similar to what Lundberg used for his targets. The experimental data, along with computational results, are shown in Fig. 20. (The solid lines connecting the actual data points are simply straight lines that connect the data points to show the penetration-time trends.)

The procedure for estimating the response of the failed material remained the same. The test at an impact velocity of 1645 m/s (Fig. 20), where dwell persists for approximately 20 μs, is used to determine the initiation of damage (the accumulated inelastic strain). This sets the failure

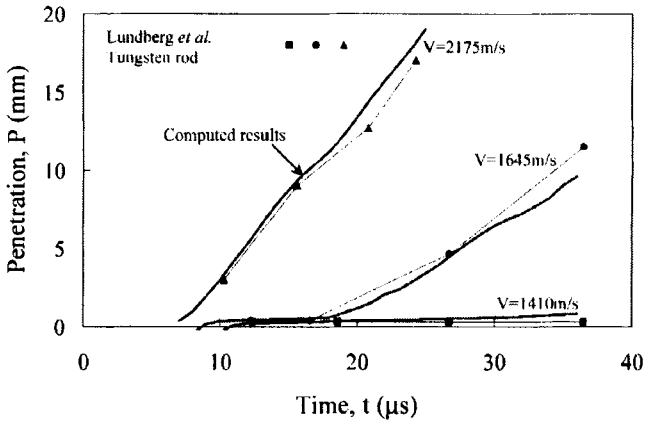


Fig. 20. EPIC simulations of Lundberg's experiments using JHB model (courtesy of T. Holmquist).

strain. The material is intact and has the strength of the intact material while damage (plastic strain) is accumulating. Upon reaching the failure strain, the material then is assumed to fail suddenly, and the response switches from the intact surface to the failed surface. After failure, the cap of the failed surface is adjusted so that the numerically calculated penetration-time response of the 1645-m/s impact matches that of the experiment. This gives a maximum value for the failed material of 0.2 GPa, which is shown in Fig. 21. The calculated curves at impact velocities of 2175 m/s and 1410 m/s in Fig. 20 use the constitutive parameters determined from the 1645-m/s impact. It is seen that the calculations predict total interface defeat at 1410 m/s, and that they show the inflection points in the penetration-time response for the 2175-m/s impact (caused by having different penetration velocities resulting from time delays in ceramic failure). The equivalent stress vs. pressure for the new model is compared to that of for the older model in Fig. 21. (The original work used the JH-1 model, which uses straight-line segments for the yield surfaces. The new work used the JHB model, which has an analytic form for the yield surfaces.)

The Drucker-Prager model, using the constants derived by Walker for SiC, has been used in CTH to reproduce the experimental data of Orphal, *et al.* [38]. These data are also reproduced using the JHB model parameters for SiC [39]. Clearly, the discrepancies between the values by Walker for SiC are dramatically at odds with those used by the J-H model. One interpretation is that the Walker-Anderson model constants represent an "averaging" of the intact and failed material response. This would seem to make some sense, but this interpretation does not allow for the relatively good agreement between the constitutive constants for failed $B_4C$ material.

It is highly desired that the constitutive constants be determined by independent laboratory experiments. SwRI has developed experimental techniques to determine response of confined SiC powder and *in-situ* damaged (comminuted) SiC [40]. The results are shown in Fig. 22, and compared to the J-H and Walker-Anderson model constants. Although an estimate of the cap has been made, there is considerable uncertainty in its value since the platens fail at the higher stress levels. There remain questions concerning the experimental procedures and the

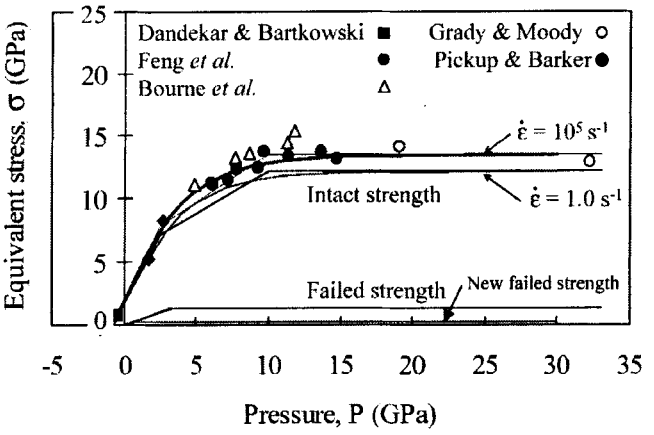


Fig. 21. Comparison of old and new SiC models with new failure surface (courtesy of T. Holmquist).

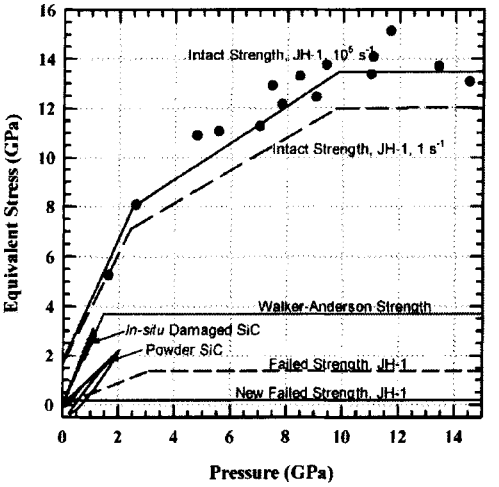


Fig. 22. Strength of comminuted and powder SiC tests compared to J-H and Walker-Anderson model parameters [40].

interpretation of the results, and on-going work is examining assumptions and interpretations. Additional research is also being conducted to refine and modify the experimental procedures, and new analysis tools are in development for the interpretation of the laboratory data. Nevertheless, the laboratory data are in approximate agreement with the Walker values. In fact, the strength of compacted SiC powder greatly exceeds that required by the JHB model to

reproduce Lundberg's experiments. Thus, notwithstanding the demonstrated success of the J-H model, questions remain.

SUMMARY

An objective of computational constitutive models is to match as many diverse and types of experiments as possible. The geometry and/or impact conditions will change for these different experiments, but the same set of constitutive model parameters should be used. This has been demonstrated quite successfully with the Johnson-Holmquist ceramics model. However, another objective is that model parameters be determined from independent laboratory characterization experiments, i.e., non-ballistic impact experiments. To date, in order to match some experimental data, some model parameters—in particular, the initiation criterion for failure and the strength of the failed material—have been determined from ballistic experiments. The J-H parameters for the strength of failed material differ considerably than those inferred by Walker (also determined by matching experimental data) and direct laboratory characterization experiments of compacted ceramic powder and *in-situ* comminuted ceramic. To complicate things even further, it is often difficult to separate numerical hydrodynamics from the constitutive model, as already mentioned for the J-H model in the conversion of elements to particles [33] (also see [41]). Work is on-going to develop revised constitutive parameters for $B_4C$ [39], and which may have to also include the effects of phase transformations, e.g., [42]. Considerable discussion has ensued about the nature of the failed surface, and it is hoped that further research will sort these differences out.

REFERENCES

[1]M. Wilkins, C. Honodel, and D. Sawle, "An approach to the study of light armor," UCRL-50284, Lawrence Livermore National Laboratory, Livermore, CA (1967).

[2]M. L. Wilkins, "Second Progress Report of Light Armor Program," UCRL-50349, Rev. 1, Lawrence Livermore National Laboratory, Livermore, CA (1976).

[3]M. L. Wilkins, "Third Progress Report of Light Armor Program," UCRL-50460, Lawrence Livermore National Laboratory, Livermore, CA (1968).

[4]M. L. Wilkins, C. F. Cline, and C. A. Honodel, "Fourth Progress Report of Light Armor Program," UCRL-50694, Lawrence Livermore National Laboratory, Livermore, CA (1969).

[5]M. L. Wilkins, R. L. Landingham, and C. A. Honodel, "Fifth Progress Report of Light Armor Program," UCRL-50980, Lawrence Livermore National Laboratory, Livermore, CA (1971).

[6]M. L. Wilkins, "Calculations of Elastic-Plastic Flow," in *Methods of Computational Physics*, Vol. 3 (B. Adler, S. Fernback, and M. Rotenberg, Eds.), Academic Press (1964).

[7]M. L. Wilkins, "Calculation of Elastic-Plastic Flow," UCRL-7322, Rev. 1, Lawrence Livermore National Laboratory, Livermore, CA (1969).

[8]J. E. Reaugh, Lawrence Livermore National Laboratory, personal communication.

[9]J. D. Walker and C. E. Anderson, Jr., "The Wilkins' Computational Ceramic Model for CTH," SwRI Report 4391/002, Southwest Research Institute, San Antonio, TX (1991).

[10]J. M. McGlaun, S. L. Thompson, and M. G. Elrick, "CTH: A three-dimensional shock wave physics code," *Int. J. Impact Engng.*, **10**, 351-360 (1990).

[11]C. E. Anderson, Jr. and J. D. Walker, "Ceramic Dwell and Defeat of the 0.30-Cal AP Projectile," *15th U.S. Army Symp. on Solid Mech.*, Myrtle Beach, SC, April 12-14 (1999).

[12]C. E. Anderson, Jr., M. S. Burkins, J. D. Walker, and W. A. Gooch, "Time-Resolved Penetration of $B_4C$ Tiles by the APM2 Bullet," *Computer Modeling in Engng. & Science*, **8**(2), 91-104 (2005).

[13]A. M. Rajendran, "Historical Perspective on Ceramic Materials Damage Models," *Ceramic Transactions, Ceramic Armor Materials by Design*, (J. McCauley, *et al.*, Eds.), **134**, pp. 281-297, The American Ceramic Society, Westerville, OH (2002).

[14]A. M. Rajendran, "Modeling the Impact Behavior of AD85 Ceramic Under Multiaxial Loading," *Int. J. Impact Engng.*, **15**(6), 749-768 (1994).

[15]A. M. Rajendran and D. J. Grove, "Determination of Rajendran-Grove Ceramic Constitutive Model Constants," in *Shock Compression of Condensed Matter—1995* (S. C. Schmidt, Ed), pp. 539-542, AIP Press, NY (1996).

[16]A. M. Rajendran and D. J. Grove, "Modeling the Shock Response of Silicon Carbide, Boron Carbide, and Titanium Carbide," *Int. J. Impact Engng.*, **18**(6), 611-631 (1996).

[17]D. J. Grove and A. M. Rajendran, "Overview of the Rajendran-Grove Ceramic Failure Model", *Ceramic Transactions, Ceramic Armor Materials by Design*, (J. McCauley, *et al.*, Eds.), **134**, pp. 371-382, The American Ceramic Society, Westerville, OH (2002).

[18]G. R. Johnson and T. J. Holmquist, "A Computational Constitutive Model for Brittle Materials Subjected to Large Strains, High Strain Rates, and High Pressures," in *Shock Waves and High-Strain Rate Phenomena in Materials* (M. A. Meyers, L. E. Murr, and K. P. Staudhammer, Eds.), pp. 1070-1077, Marcel Decker, NY (1991).

[19]G. R. Johnson, T. J. Holmquist, J. Lankford, C. E. Anderson, and J. Walker, "A Computational Constitutive Model and Test Data for Ceramics Subjected to Large Strains, High Strain Rates, and High Pressures," Report DE-AC04-87AL-42550/1, Honeywell, Inc., Brooklyn Park, MN, August (1990).

[20]G. R. Johnson and T. J. Holmquist, "An Improved Computational Constitutive Model for Brittle Materials," in *High-Pressure Science and Technology—1993*, (S. C. Schmidt, J. W. Shaner, G. A. Samara, and M. Ross, Eds.), 981-984, AIP Conf. Proc. 309, AIP Press, NY (1994).

[21]G. R. Johnson and T. J. Holmquist, "Response of Boron Carbide Subjected to Large Strains, High Strain Rates, and High Pressures," *J. Appl. Phys.*, **85**(12), 8060-8073 (1999).

[22]T. J. Holmquist and G. R. Johnson, "Response of Silicon Carbide to High Velocity Impact," *J. Appl. Phys.*, **91**(9), 5858-5866 (2002).

[23]T. J. Holmquist and G. R. Johnson, "Ceramic Dwell and Interface Defeat," *Ceramic Transactions, Ceramic Armor Materials by Design*, (J. McCauley, *et al.*, Eds.), **134**, pp. 485-498, The American Ceramic Society, Westerville, OH (2002).

[24]T. J. Holmquist and G. R. Johnson, "Modeling Prestressed Ceramic and its Effects on Ballistic Performance," *Int. J. Impact Engng.*, **31**, 113-127 (2005).

[25]T. J. Holmquist and G. R. Johnson, "Characterization and Evaluation of Silicon Carbide to High Velocity Impact," *J. Appl. Phys.*, **97**(09), 093502/1-12 (2005).

[26]J. D. Walker and C. E. Anderson, Jr., "An Analytic Model for Ceramic-Faced Light Armor," *Proc. 16th Int. Symp. on Ballistics*, Vol. 3, pp. 289-298, San Francisco, CA (1996).

[27]J. D. Walker and C. E. Anderson, Jr., "An analytic penetration model for a Drucker-Prager yield surface with cutoff," *Shock Compression of Condensed Matter—1997*, S. C. Schmidt, Eds., 897-900 (1998).

[28]J. D. Walker, "Analytic Model for Penetration of Thick Ceramic Targets," *Ceramic Transactions, Ceramic Armor Materials by Design*, (J. McCauley, *et al.*, Eds.), **134**, pp. 337-348, The American Ceramic Society, Westerville, OH (2002).

[29]J. D. Walker, "Influence of Drucker-Prager Constitutive Parameters on Penetration of Thick Ceramic Targets," *Proc. 20th Int. Symp. on Ballistics*, **2**, 794-801, DES*tech* Publications, Lancaster, PA (2002).

[30]J. D. Walker, "Analytically Modeling Hypervelocity Penetration of Thick Ceramic Targets, *Int. J. Impact Engng.*, **29**, 747-755 (2003).

[31]D. L. Orphal, R. R. Franzen, A. C. Charters, T. L Menna, and A. J. Piekutowski, "Penetration of Confined Boron Carbide Targets by Tungsten Long Rods at Impact Velocities from 1.5 to 5.0 km/s, *Int. J. Impact Engng.*, **19**(1), 15-29 (1997).

[32]D. L. Orphal and R. R. Franzen, "Penetration of Confined Silicon Carbide Targets by Tungsten Long Rods at Impact Velocities from 1.5 to 4.6 km/s," *Int. J. Impact Engng.*, **19**(1), 1-13 (1997).

[33]G. R. Johnson, S. R. Beissel, and T. J. Holmquist, "Improved Computational Modeling of Ballistic Problems using Meshless Particles and Finite Elements," *Proc. 20th Int. Symp. on Ballistics*, **2**, 850-858, DES*tech* Publications, Lancaster, PA (2002).

[34]T. J. Holmquist, D. W. Templeton, and K. D. Bishnoi, "Constitutive Modeling of Aluminum Nitride for Large Strain, High-Strain Rate, and High-Pressure Applications," *Int. J. Impact Engng.*, **25**(3), 211-232 (2001).

[35]T. J. Holmquist, D. W. Templeton, and K. D. Bishnoi, "High Strain Rate Constitutive Modeling of Aluminum Nitride including a First-Order Phase Transition," *J. Phys., IV*, France **10**, Pr9/21-26 (2000).

[36]G. R. Johnson, T. J. Holmquist, and S. R. Beissel, "Response of Aluminum Nitride (including a Phase Change) to Large Strains, High Strain Rates, and High Pressures," *J. Appl. Phys.*, **94**(3), 1639-46 (2003).

[37]P. R. Lundberg, R. Renstrom,and B. Lundberg, "Impact of Metallic Projectiles on Ceramic Targets: Transition Between Interface Defeat and Penetration," *Int. J. Impact Engng.*, **24**, 259-275 (2000).

[38]D. L. Orphal, C. E. Anderson, Jr., D. W. Templeton, Th. Behner, V. Hohler, and S. Chocron, "Using Long-Rod Penetration to Detect the Effect of Failure Kinetics in Ceramics," *Proc. 21st Int. Symp. on Ballistics*, pp. 744-751, Adelaide, Australia, 19-13 April (2004).

[39]T. J. Holmquist, personal communication.

[40]S. Chocron, K. A. Dannemann, A. E. Nicholls, J. D. Walker, and C. E. Anderson, Jr., "A Constitutive Model for Damaged and Powder Silicon Carbide," *Proc. 29th Int. Conf. Advanced Ceramics & Composites, Ceramic Engng. & Sci. Proc.*, **26**(7), 35-42, American Ceramics Society (2005).

[41]C. E. Anderson, Jr., I. S. Chocron, and C. E. Weiss, "Analysis of Time-Resolved Penetration of Long Rods into Glass Targets—II," *30th Int. Conf. & Exp. on Advanced Ceramics and Composites*, The American Ceramics Society, Cocoa Beach, FL, 22-27 Jan. (2006).

[42]M. Chen, J. W. McCauley, and K. J. Hemker, "Shock-Induced Localized Amorphization in Boron Carbide," *Science*, *299*, 1563-1566 (2003).